Curr Radiol Rep (2015) 3:9
DOI 10.1007/s40134-015-0090-3

Dual-Energy CT: Applications in Abdominal Imaging

Ralf W. Bauer · Sebastian Fischer

Published online: 12 February 2015

Abstract Dual-energy CT (DECT) is a steadily emerging innovative imaging modality. Various applications have been developed and applied to successfully solve diagnostic difficulties that standard CT has in the abdomen. This includes kidney stone differentiation, cholesterol gallstone detection, renal and adrenal lesion characterization, and tumor response monitoring. This article is supposed to give a current update on possible applications of DECT in the abdomen and their evidence.

Keywords Dual-energy CT · Imaging modality · Abdomen

Introduction

Eight years after the first dual-source dual-energy CT (DECT) device usable for clinical routine work had been introduced to the market, we have just faced the launch of the third generation of this scanner class underlining that the once new kid on the block has come to stay. Besides the dual-source approach, the concept of rapid kV switching has established itself as the second big player in the field, with two serial helical acquisitions at different kV levels and the "sandwich detector" technology currently still exploiting their technical and clinical potential. The number of peer-reviewed publication on the use of DECT for abdominal imaging has sky rocked especially in the last 3–4 years indicating the deep interest in this still novel technique. The vast amount of literature makes it difficult to get the essentials, especially for somebody to start off in that field. This review article will give a short insight into physical and technical aspects of DECT, but will mainly focus on current evidence for its organ- and pathology-specific use in the abdomen.

This article is part of the Topical Collection on *Abdominal CT-An Update on Applications and New Developments*.

R. W. Bauer (✉) · S. Fischer
Department of Diagnostic and Interventional Radiology, Clinic of the Goethe University Frankfurt, Haus 23C UG, Theodor-Stern-Kai 7, 60596 Frankfurt, Germany
e-mail: ralfwbauer@aol.com

Technical Background

Physical Principles

The attenuation of X-rays by a certain material depends on largely three factors: (a) the effective atomic number of that material, (b) its physical density, and (c) the energy (keV) of the X-ray interacting with it. The higher the effective atomic number and the lower the X-ray energy, the higher the attenuation displayed in HU. This change is characteristic for every material and hence allows discriminating different materials and tissues [1•, 2]. While soft tissues usually are composed of hydrogen, oxygen, and carbon with low effective atomic numbers, e.g., bone contains calcium with higher atomic number. Above that, we have iodine that displays a very strong dual-energy effect at kV levels used in diagnostic CT (80–140 kV) [1•, 2]. This is a good basis to subtract or highlight iodine-specific signal in an image. In CT, interaction of X-rays with matter is usually defined by the photo effect and Compton scattering. The photo effect occurs at lower energies and will eject a k-shell electron from its shell. Compton scatter occurs at higher energies and interacts with outer-shell electrons where both the X-ray and the electron change their direction and energies after

interaction. The photo effect is the more relevant one in diagnostic CT. The closer the X-ray energy comes to the absorption maximum, so called k-edge energy, the higher the attenuation of that material will be [1•, 2].

Hardware

Currently, there are mainly two concepts fit to be used in clinical routine: the one is the dual-source (DS DECT) concept (Siemens Somatom Definition DS, Somatom Definition Flash, and Somatom Force), the other one is the single-source rapid kV-switching (rkVs) concept (GE Discovery CT 750 HD and Revolution). For the dual-layer detector approach and sequential acquisition of two consecutive separate spiral scans at high and low kV, no resilient data are available and hence we will not focus on them. The dual-source concept has two X-ray tubes and corresponding detector banks mounted onto the same gantry. This enables almost simultaneous sampling of the same voxel at high and low tube potential. By spatial restrictions, one detector needs to be smaller than the other one (one detector with a full standard 50 cm FOV, another detector with a significantly smaller FOV of 26, 33, or 35 cm for Definition DS, Flash and Force, respectively). Dual-energy information is only available within the smaller FOV, which lead to restrictions in abdominal imaging with first-generation DS DECT since most organs are usually not fully covered within 26 cm. For improved cross-scatter correction, it was mandatory to use a 14×1.2 mm collimation in the abdomen with first-generation DS DECT [3]. Improvements in software-based cross-scatter correction with the second and third generation DS DECT allow for using the minimum collimation of $32–128 \times 0.6$ mm with improved spatial resolution. Tube potential is fixed at 80 and 140 kV on first-generation. On second-generation, it can be chosen from 80 and 100 kV on tube A with fixed 140 kV with additional hardening of the polychromatic spectrum by a 0.4 mm tin filter (Sn) on tube B. With the third-generation, the high kV is fixed at 150 kV with Sn filter while for the low kV it can be chosen from 70 to 100 kV. Adding a tin filter to the high kV tube will result in filtration of low-energy photons left of the mean energy peak and hence result in an effective hardening of the mean energy of the polychromatic spectrum [4]. The mean energies of the high and low kV spectrum are further separated with less overlap which improves tissue differentiation. It further reduces patient dose since these low-energy photons generated at the high kV tube do not contribute to image impression but only to exposure. The second big benefit with second-generation DSCT is that 100 kV can be selected on tube A to have a more penetrable spectrum available for abdominal imaging resulting in less noise and requiring less restrictive selection of patients according to their body habitus. In combination with the tin filter on the 140 kV tube, the spectral differentiation is not hampered. A big benefit with third-generation DSCT now is the relevantly increased tube capacity that, in turn, allows using lower kV levels on tube A, again.

The rapid kV-switching approach resembles a standard CT device with only one tube and corresponding detector with full 50 cm FOV. However, the tube is capable of rapidly switching the potential several thousand times per rotation. This requires a very fast reacting detector material with ultra-short afterglow (Gemstone, GE). Here, 80 and 140 kV are used without additional Sn filtration of the 140 kV spectrum, which is technically not feasible at such fast kV-switching periods. DE-specific processing of data is performed after image reconstruction from the raw data on DS DECT and is done from the source raw data in projection space on kV-switching DECT.

Software and Image Processing

Both Siemens and GE offer their own dual-energy processing software, either as classical workstation or server-based (GE Gemstone Spectral Image Viewer on AW Server or Advantage Workstation; Siemens Dual Energy CT on Syngo Via server or MMWP). There, it can be chosen from a bunch of dedicated algorithms. A major drawback is that the dual-energy applications are not yet integrated on the scanner console. It is desirable to have dual-energy specific tasks such as the generation of virtual un-enhanced (VUE) images, iodine maps, or mono-energetic reconstructions readily available there. This would speed up the workflow and lead to bigger usage of DE-specific data by radiologists during normal reading on a PACS workstation.

The processing of dual-energy data is always based on the principle of material decomposition. Siemens uses the so-called three material decomposition (e.g., for most abdominal application with contrast enhancement this would be soft tissue, fat and iodine as the baseline materials as in the LiverVNC algorithm), GE the basis pair decomposition (e.g., water–iodine, fat–iodine, etc.). At the end, with either approach it is feasible to generate images in which the iodine information is subtracted (VUE or water images) or to display solely the iodine information and distribution (iodine distribution/overlay/density or perfusion maps). Since calcium is not included in these decomposition algorithms typically used for the contrast-enhanced CT of the abdomen, calcifications may erroneously be partially removed in VUE data sets [5]. Virtual non-enhanced images tend to be smoother than TUE images due to some specific steps in image generation. The image impression was generally different from TUE scans which led to problems with acceptability, especially with first-generation DS

DECT. With advances in image processing, the image impression of VUE has more and more become similar to TUE images. Now with the regular use of iterative reconstruction, there is almost no perceivable difference any more. Initially, iodine quantification in mg/ml was a feature exclusive to GE, but has now been available with Siemens software, too. Likewise, enhancement can be measured in HU, but ROI measurements will exclusively contain enhancement due to iodine content without disturbance of underlying maybe heterogenic native density values as they can be found in hemorrhagic cysts or tumors. Gray scale images can further be generated by mixing high- and low-kV source data linearly in steps of 1 % or non-linearly according to a changeable sigmoid curve where center and width are freely chosen (exclusive to Siemens). Both vendors offer the calculation of interpolated, virtual mono-energetic images in a range between 40–140 keV (GE) or 40–190 keV (Siemens). These images generate an image impression as if the X-ray beam had only photons of one single energy. Extrapolation to higher keV can be used to suppress iodine enhancement (pseudo-unenhanced images) or reduce metal artifacts, extrapolation toward lower keV can increase iodine-related enhancement and, hence, increase tumor-to-organ or vessel contrast. The further the simulated keV image moves away from the mean peak energy of the poly chromatic source beam, the higher image noise will be, since only very little true information of photons of these very high or low energies is there. Currently, Siemens has found a way to overcome that issue and preserve low image noise from the virtual polychromatic 120 kV image and combine it with the benefit of higher attenuation at lower keV (so-called mono-energetic plus) [6••, 7]. GE uses its adaptive statistical iterative reconstruction (ASIR) to reduce noise in mono-chromatic images.

Dose Considerations

Still discussions go on if DECT goes along with a "dose penalty" compared to a 120 kV standard protocol or if it may be dose neutral. Generally, literature on this point is scarce. Studies empirically compared CT dose parameters from patient cohorts scanned with a single energy protocol to the same or a different cohort scanned with a DE protocol with tube settings as suggested by the manufacturer or customized [8, 9]. The more relevant approach would be to set tube parameters in a way that the same image quality is achieved and then look at the dose parameters necessary to achieve that goal. From the physical background, DE data processing will function better with lowest image noise since noise determines how accurate the CT value of a voxel is. However, reliable results are achieved with tube settings that respect diagnostic reference values suggested by authorities for abdominal CT. From our own experience with three generations of DS DECT, we can tell that very good DE data processing is achieved when protocols are designed CTDIvol-equivalent to the comparative and competitive single-energy standard protocol. The dual-source concept has the advantage that automated exposure control (topogram-based and angular mA modulation) can be used to individually adjust tube output and keep image quality constant. The rkVs concept cannot adapt mA together with the kV by physical restrictions leading to "overexposure" at high kV. However, one is free to reduce the suggested mA values to the specific diagnostic task and individual patient size. Further, the manufacturer has created concepts to acquire more projections at low kV than at high kV reducing the relative contribution of high-energy X-rays to keep CTDIvol in a reasonable range.

Clinical Applications

Liver

Although the definite value of including a non-enhanced phase into a standard liver CT protocol is not completely clear, many institutions worldwide perform it followed by a later arterial and venous phase, and, depending on the task, a delayed phase as well. The native phase has advantages in showing focal spots of calcifications, assessing fatty liver or showing attenuation changes suggestive of iron depositions. However, it may not be required in every case as a standard. Hence, interest has been great in deriving VUE images from contrast-enhanced DE data for liver CT.

With first-generation DS DECT Zhang et al. reported that VUE images derived from arterial phase liver CT were superior to those derived from portal venous phase in terms of HU stability [10]. Although HU values were not significantly different from TUE, image impression was not rated the same. Rim artifacts, incomplete subtraction of iodine and subtraction of calcifications, and lipiodol were reported. De Cecco et al. found largely good diagnostic image quality for VUE images derived from DE portal venous phase, however, also with restrictions in some cases due to artifacts [11]. Both applied a BMI restriction (>40 and >35 kg/m^2). With a study on second-generation DS DECT with 80/140 kV Sn configuration De Cecco et al. found high HU deviations for liver, spleen, or kidney cortex, which was even more pronounced in arterial phase than in portal venous phase [12]. Subjective image quality rating did also not reach the level of TUE. The problem of subtraction of calcified lesions and some surgical clips and incomplete iodine subtraction (with artificially better depiction of hypodense liver lesions) remained. They concluded that VUE cannot fully replace TUE. These

observations are in line with Sahin et al. [13••]. Barrett et al. conversely found only minimal HU differences in the abdomen when using the 100/140 kV Sn configuration, with VUE images derived from portal venous phase performing a little bit better than those from arterial phase [14]. Known typical image artifacts were described as well. Toepker et al. found higher HU deviations with 100/140 kV Sn, especially in very low attenuating tissues like fat or structures with high iodine content as spleen or aorta [15]. However, in average 75 % of all measurements between VUE and TUE were within an absolute deviation of 10 HU. These findings are supported by Kaufmann et al. [16].

Miller et al. introduced a way how these variations can be minimized by individually adjusting the input parameters of the material decomposition parameters to the specific patient attenuation values [17]. With this method, they were able to achieve significantly smaller deviations of HU values of the VUE compared to the TUE series, with less than 10 HU difference.

Depicting focal liver lesions is a major task of CT. However, MRI with its way superior soft tissue contrast is much better to detect and characterize even small lesions. Hence, DE-specific imaging features have been investigated in hypo- and hypervascular liver lesions. Three studies on HCC with kV-switching late arterial phase DECT independently report that mono-chromatic images at 50 keV provide best tumor-to-liver contrast, best subjective image quality and improved lesion detection rate and confidence [18, 19•, 20]. Yamada et al. found that the highest tumor-to-liver contrast for hypovascular lesion in portal venous phase was between 66 and 71 keV [21]. Kim et al. were able to show that non-linear blending is superior to linear blending in terms of image quality for the detection of HCC with first-generation DS DECT [22].

Adequate depiction of hepatic vascular anatomy is challenging in conditions like heavy cirrhosis with shrunk or chronically occluded portal vein and varicosis and altered hemodynamics. Likewise ascites or large amounts of abdominal fat reduce image quality substantially. DECT has been successfully applied for improving hepatic and portal vein contrast and the quality of CT angiography by non-linear blending and virtual mono-energetic reconstructions with significantly superior results than standard 120 kV acquisitions [23–27].

Optimization of image contrast with mono-energetic or non-linear blending has also been shown to be feasible with 37–50 % reduced iodine amount. Image quality was preserved or even improved with good lesion contrast and gain in vascular enhancement. Potential benefits in patients with reduced kidney function have been discussed [28, 29••].

DECT has further been used for quantifying fatty liver (in both native and contrast-enhanced scans) [30, 31] and iron overload [32] with very high accuracy. Approaches were either based on HU differences at higher and lower photon energies or quantitative measurements of fat and water content on kV-switching DECT.

Biliary Tract

Experience with DECT for imaging the biliary tract and its pathologies is scarce. The technique has only been applied for gallstone detection and characterization and CT cholangiography in healthy donors before liver transplantation—all studies performed on the first generation of DS DECT.

Gallstones with high cholesterol content usually elude detection on standard 120 kV abdominal CT as this type of stones appears isodense to gallbladder fluid. In an in vitro experiment, we were able to enhance the detection rate of stones with high cholesterol content and no calcifications with the help of the 80 kV series and to determine the characteristic spectral behavior of such pure cholesterol stones at high and low kV [33]. By means of that, cholesterol stones could be identified as such with 95 % sensitivity and 100 % specificity. In another in vitro study, Voit et al. were able to achieve 100 % diagnostic accuracy for any type of stones (calcified, pigment, cholesterol) by additionally color-coding the spectral information of different stone types [34]. However, no such data exists for newer scanner generations and up to date no patient study to confirm these results is available (Fig. 1).

CT cholangiography is an alternative to invasive ERCP or MRCP in patients with contraindication to these procedures. However, the demand for special ionic iodinated contrast agents excreted via the biliary system and their high allergoid potential with adverse events regularly observed has led to the fact that this examination nowadays has largely disappeared and is mostly conducted in dedicated centers only. Sommer et al. [35] and Stiller et al. [36] shared their experience in healthy liver donors that underwent CT cholangiography in DE mode. Both authors found image quality parameters SNR and CNR to be excellent in the 80 kV source data images, because the higher inherent image noise is compensated for by the increased iodine contrast. Hence image quality parameters were not inferior to the virtual 120 kV images. Both authors conclude that in case DECT is not available, CT cholangiography should preferably be conducted at 80 kV and low tube current with the potential to save radiation dose. When quantitative analysis becomes important, Sommer et al. recommend using DE reconstructed data for more precise measurements through profiting from dedicated iodine beam-hardening correction. Here, non-linearly blended images of high and low kV information and pure iodine images performed superior to virtual 120 or 80 kV images alone (Fig. 2).

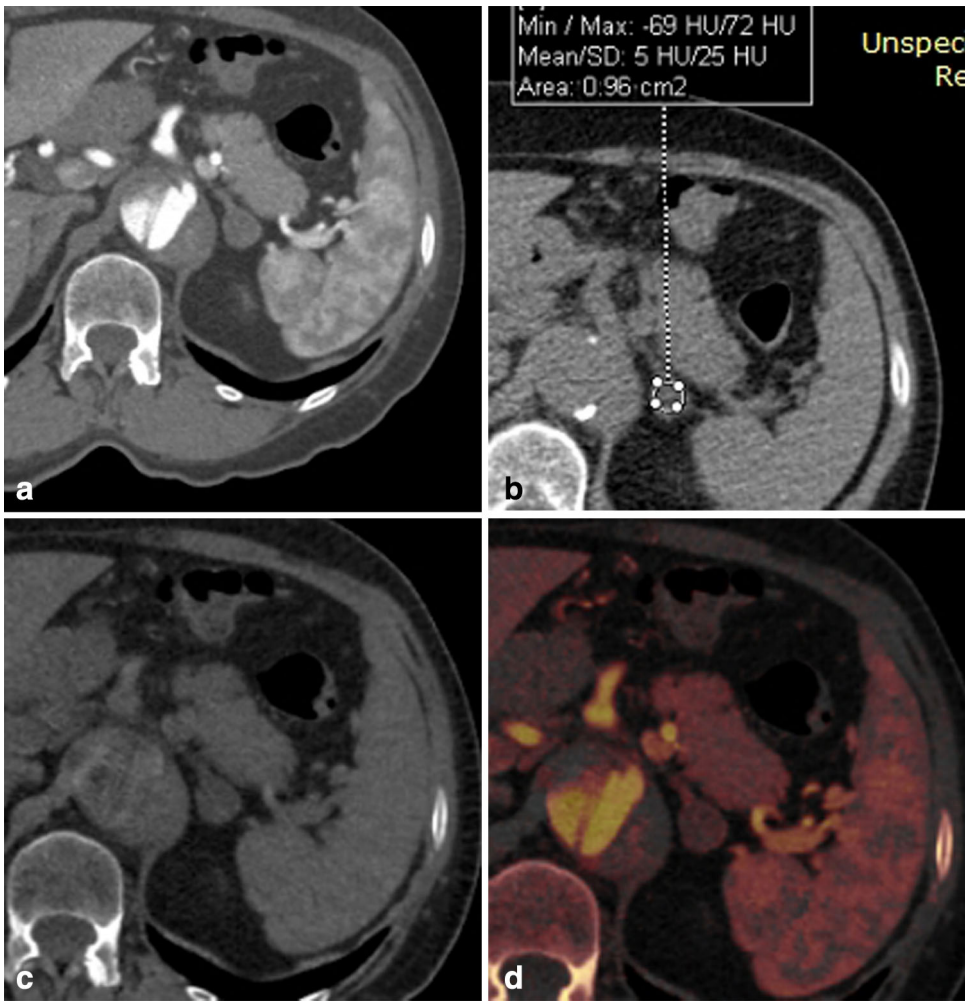

Fig. 1 Incidental finding of a 1.4 cm big mass in the left adrenal gland on DECT angiography for suspected type B dissection. The native scan shows a mean density of the mass of 5 HU (**a**). VNC images were derived from the angiographic phase with well correlating image impression. Note some artifacts around the dissection membrane (**b**). Color-coded iodine overlay images in arterial phase show a iodine-based enhancement of the lesion of 36 HU and a native density after iodine subtraction of 6 HU (**c**, **d**)

Pancreas

CT of the pancreas is mainly conducted with the question for pancreatitis or pancreatic mass. Currently, no evidence is available that DECT is beneficial in terms of a more accurate delineation of vital, perfused pancreatic remainder tissue in acute necrotizing pancreatitis or better appreciation of fluid collections, necrosis, or abscess formations—both important features to predict patient outcome according to various CT severity indices. Likewise, there is currently no published evidence that DECT could help to differentiate between acute focal pancreatitis and adenocarcinoma which both typically present as focal hypo-attenuating mass with delayed contrast wash-in compared to normal pancreatic tissue.

At first presentation of a patient with suspected pancreatic pathology one may typically use a triple phase scan protocol consisting of an un-enhanced, late arterial, also known as pancreatic parenchymal, and a hepato-venous phase. The native phase is usually used to screen for focal calcifications and concrements or to determine the native density of focal cystic lesions. Mileto et al. investigated the reliability of VUE images generated from late arterial phase in comparison to TUE images on a first-generation DS DECT [37]. Although the observers found the general image quality of the VUE images to be not significantly different from the TUE images, they reported on two cases in which the VUE algorithm falsely subtracted calcifications and on one case in which a plastic bile duct stent was erroneously removed. Although the authors concluded that with discard of the TUE scan an average dose reduction of 27 % was feasible, the inconsistent quality of VUE images may not justify this approach in patients at initial presentation with first-generation DS DECT.

Patel et al. were the first to report their initial results on spectral CT with kV switching in 64 patients with pancreatic adenocarcinoma [38]. Compared to 70 keV images, that resemble the image impression of a polychromatic spectrum at 120 kV, tumor-to-pancreas contrast significantly improved on 45 keV mono-chromatic images and on individually calculated "optimal CNR" images which laid around 50–52 keV. However, looking at CNR values only, the absolute differences were marginal and did not reach statistical significance, which is most likely due

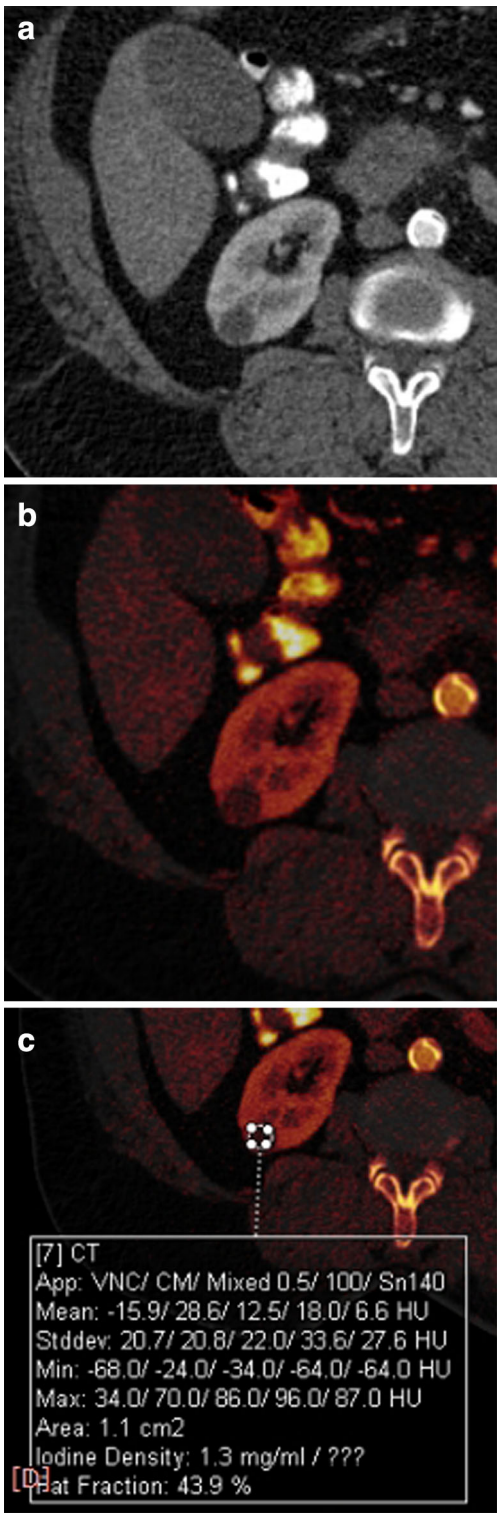

Fig. 2 Incidental finding of a 1.2 cm big hypodense lesion in the right kidney on DECT angiography of the abdominal aorta. The *lesion* shows a somewhat pixilated texture consistent with small vessels. DE-based quantification reveals a virtual un-enhanced density of −15 HU with a fat fraction of the lesion of 43 %. Iodine uptake was 1.3 mg/ml. Biopsy showed angiomyolipoma

to the dramatically higher noise when virtual keV values decrease (noise at 70 keV 23.6 HU, at 45 keV 58.9 HU). Our group has been looking into benefits with an advanced noise-optimized mono-energetic reconstruction algorithm with second-generation DS DECT for improving the conspicuity of pancreatic adenocarcinoma and has found that noise at lower extrapolated keV can be stabilized at values of the virtual 120 kV blended series. Hence, this will directly translate into improved CNR at lower energy levels such as 40 and 55 keV and better lesion delineation.

If mono-energetic images at low photon energies with or without noise-optimized algorithms or iodine maps may be capable of actually improving the detection of pancreatic adenocarcinoma isodense to normal pancreas or intraductal carcinoma is yet to be shown. Lin et al., however, were able to show improved diagnostic accuracy of pancreatic insulinoma—a difficult to diagnose, typically hyperperfused tumor with early contrast material wash-in and rapid wash-out—with kV-switching DECT [39•]. The detection rate for lesions was improved from 68.8 % with standard 120 kV 64-slice CT to 95.7 % with a combined approach of mono-chromatic images at 70 keV and iodine maps (Fig. 3).

Adrenal Glands

Focal lesions of the adrenal glands are a frequent finding on CT. In an unselected general population, the chances for malignancy—especially for primary adrenal tumors such as pheochromocytoma or adrenal cortical carcinoma—are very low. In a pre-selected, oncological population the likelihood for these focal lesions being metastasis significantly increases. The appraisal of such a lesion as benign or malignant has major impact on the patient's further management. CT per se is a very good diagnostic tool to characterize adrenal lesions with the help a triple phase protocol consisting of an un-enhanced, an early contrast phase ($\sim$60 s after contrast injection), and a delayed phase scan (10 or 15 min after contrast injection) by considering native density and wash-out characteristics. Adenomas will typically show a native density of max. 10 HU due to their high lipid content with rapid contrast wash-in and early wash-out (approx. 50 % HU decay in the delayed scan), whereas malignant lesions typically present with a native density of >20 HU and delayed wash-out (<50 % HU decay in the delayed scan). The lipid-poor adenomas may represent a challenging etiology since their native density may lie between 10 and 30 HU, but with the help of contrast dynamics, surveillance of size and consideration of patient history the majority of these lesions will also be characterized correctly (Fig. 4).

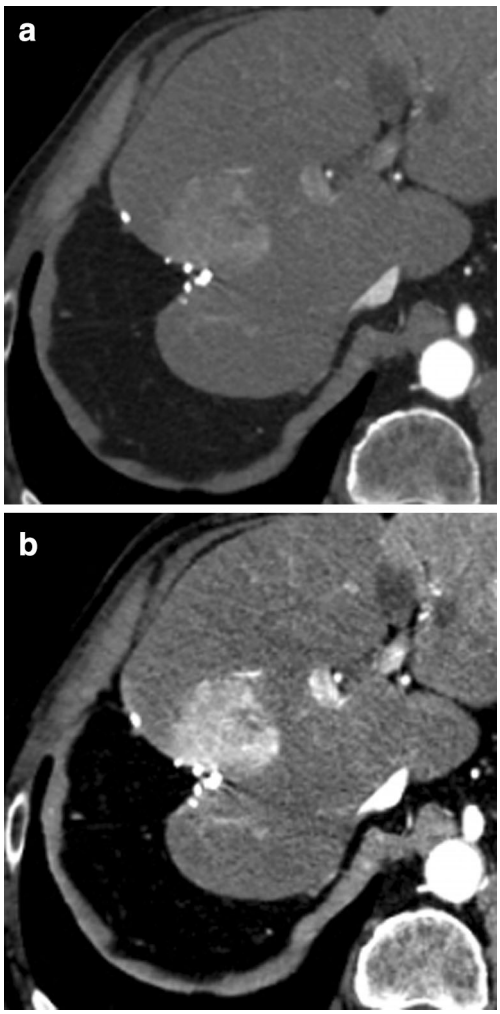

Fig. 3 A follow-up CT in a patient with right hemihepatectomy shows a 3 cm big hyperperfused mass in arterial phase at the resection margin of the remaining left liver. **a** Shows the 70 keV mono-energetic plus image, **b** the 40 keV mono-energetic plus image. Note the markedly increased lesion-to-liver contrast at still low noise levels of 23 HU resulting in superior CNR and image quality at 40 keV

Attempts have been made with DECT as to compare VUE to TUE images in terms of HU consistency or to use its capability of improved chemical decomposition of tissues. Gnannt et al. [40] and Ho et al. [41] were the first to publish their initial experiences in small case series of patients with focal adrenal lesions with first-generation DS DECT. Mean HU of TUE and VUE were not significantly different in both patient cohorts with VUE tending to overestimate lesion density a bit (by 1–2 HU in average). While with Ho et al. up to three adenomas were classified as >10 HU on VUE, no metastasis was misclassified as benign [41]. Gnannt et al. reported on one case with severe artifacts of the VUE not allowing sufficient diagnosis [40]. Diagnostic agreement was good to very good in both publications (83–91 % Ho,

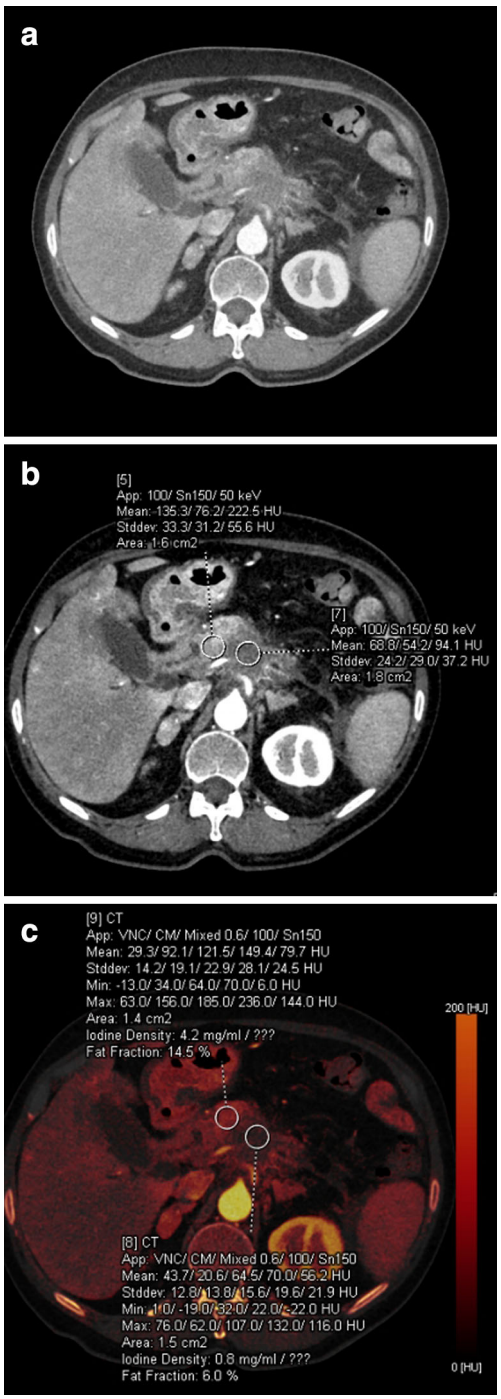

Fig. 4 In a patient suspected of having pancreatic carcinoma DECT identified a 4 cm big hypodense mass in the pancreatic corpus surrounding the celiac trunk and having contact to 1/3 of the superior mesenteric artery. The portal vein was occluded with no thrombus material left but with beginning cavernous transformation encasing the dilated common bile duct. Note the markedly increased tumor-to-pancreas contrast at 50 keV mono-energetic plus images (**a**) compared to the linearly blended image giving the impression of a standard 120 kV acquisition (**b**). Iodine distribution maps confirm the reduced tumor vascularity compared to healthy pancreas (**c**)

78–97 % Gnannt) and best in lesions measuring >1 cm. In a recent study with DS DECT of the second generation with 80 and 140 kV Sn filter, Kim et al. investigated the accuracy of VUE images derived from an early and late contrast-enhanced scan with a triple-phase adrenal protocol [42]. They concluded that iodine subtraction was incomplete in the early enhancement series resulting in significantly higher CT values in that VUE images than with TUE or VUE values derived from the delayed scan. Especially, the sensitivity for lipid-rich adenomas was poor (100 % on TUE, 38.9 % on VUE from early enhancement and 61.1 % from delayed enhancement scans). However, adding the information from contrast dynamics, the protocol based on VUE was not significantly inferior to the one based on TUE (sensitivity 100 % for both, specificity 87.5 % vs. 93.8 %). Omitting the TUE phase would have resulted in a reduction of the total DLP of 27 %. However, if this approach is overall more practical or more beneficial in a test that has a very high diagnostic accuracy per se when conducted in the standard way remains open. Kim et al. further missed to discuss the fairly large discrepancy of their results achieved with the actually newer, technically superior DS DECT device of the second generation when compared to Gnannt's and Ho's results.

Gupta et al. used two consecutive un-enhanced scans at 80 and 140 kV to look at attenuation change of lipid-rich and lipid-poor adenomas and metastases [43]. They were able to increase the specificity for the characterization of adrenal lesions on TUE images: while metastases show an attenuation increase on 80 kV (~9 HU), there is almost no change (~0 HU) or rather a decrease at 80 kV for adenomas, especially for lipid-rich ones. While the previously cited studies included virtually only a hand full of metastases, in the population of Shi et al. nearly one-third of lesions (21 of 63) were metastases [44•]. Un-enhanced DE scans were performed with a second-generation DS DECT at 80 and 140 kV and mono-energetic extrapolation without advanced noise-reduction was used for post-processing. In contradiction to Gupta, Shi reported almost no change of attenuation of metastases between high and low kV and 40 and 100 keV with markedly decreased HU values at 80 kV and 40 keV compared to 140 kV and 100 keV for adenomas, especially for lipid-rich ones. However, mono-energetic parameters did not improve diagnostic accuracy over high and low kV CT values alone. In front of the ambivalent results from these two papers, a definite conclusion on the usefulness of un-enhanced DECT for adrenal mass differentiation by HU measurements cannot be drawn.

Morgan et al. tried to clarify the usefulness of material density images and mono-chromatic images at high photon energy (140 keV) for differentiating high- from low-lipid content adrenal nodules with kV-switching DECT [45]. DE scans were obtained in late arterial phase and, conversely to other studies, adrenal hyperplasia and adenomatous hyperplasia as well as myolipoma were included. HU values at 140 keV, where the influence of iodine on CT values is minimized, correlated best with TUE CT values ($r = 0.946$) followed by the material decomposition pairs fat–iodine ($r = 0.933$) and water–iodine ($r = 0.929$). If a specificity of 94 % was desired to be achieved, the threshold for fat–iodine would be 987 mg/ml. However, none of the DE-derived characteristics was able to differentiate between lipid-poor adenoma and metastasis. A general limitation of their study is the small sample size with only 12 adenomas (4 lipid-poor) and 8 malignant lesions. In the most recent study, Mileto et al. were the first to find higher diagnostic accuracy with kV-switching DECT and material density analysis than with the classic parameter CT density on TUE images [46]. While TUE series achieved a sensitivity of 67 % only for the correct classification of adenomas, with the help of fat–iodine, iodine–fat, water–fat, and fat–water basis pair discrimination this value could be increased to 96 % at 100 % specificity. Noteworthy, even lipid-poor adenomas were reliably distinguished from non-adenomas in a more homogenously distributed cohort with 24 adenomas (8 of them lipid-poor) and 23 non-adenomas. All four investigated basis pairs performed equally well, e.g., revealing a fat–iodine value of 997 mg/ml as one possible discriminator.

Kidneys and Urinary Tract

Renal Mass

Just as with characterization of adrenal lesions, the correct classification of renal masses depends on native CT density on the one hand side, and on the level of contrast enhancement on the other hand side. Together with morphological features like the presence of macroscopic fat, calcifications, septa, and wall thickness decisions with high validity can be made whether a lesion is most likely benign or malignant with usually few equivocal cases requiring further testing. A mainstay of this diagnostic pathway is the incorporation of a non-enhanced baseline phase. Hence, renal imaging has been in the focus of dual-energy researches from the very beginning. Graser et al. were the first to find that VUE CT values derived from DECT in nephrographic contrast phase do not significantly differ from TUE CT values and concluded that the native phase could be omitted with correspondent dose savings [47]. Their work was conducted on a first-generation DS DECT in 110 patients, where in only three cases image quality of VUE images was not accepted for diagnosis by two radiologists. Artifacts were reported in up to 23 % of cases and consisted of false subtraction of calcium, rim artifacts, or beam-hardening. Neville et al. were able to support those observations with no statistically significant difference between TUE and VUE but with a tendency to slightly higher

values with VUE [48]. However, none of the lesion in their 139 patients with simple and hemorrhagic cysts, solid masses, and angiomyolipomas would have been classified differently. Graser et al. were further the first to compare the traditional way of reading renal CT with TUE and nephrograpic gray scale images to the DE way with VUE images and color-coded iodine distribution maps only [49••]. DE-specific region of interest measurement were used to determine the iodine-based lesion enhancement. They found that with the DE-specific approach the average reading time could be reduced by more than 1 min and that reading is more intuitive when it comes to decide about enhancement. Diagnostic accuracy in 202 patients was not significantly different between both ways (DE 94.6 %, standard 96 %) and hence the authors concluded that a single DE nephrographic phase would be sufficient. In only two cases, VUE image quality was rated as poor. These findings were confirmed by Song et al. in a study with 60 patients, also performed on a DS DECT scanner of the first generation [50]. And also Ascenti et al. found color-coded iodine maps to increase the level of confidence in the decision on contrast enhancement of complex renal cysts over the standard approach with TUE and gray scale images [51]. They reported on two cases with false subtraction of calcifications from renal lesions, too. The overall image quality of TUE images was rated slightly, but significantly better than that of VUE images.

The first publication on kV-switching DECT was presented by Kaza et al. and this group took a look at iodine quantification as the central decisive criterion of lesion enhancement [52•]. While in 39 patients with 20 enhancing lesions VUE ("water image") combined with iodine only images were more specific, color-coded iodine overlay images were more sensitive with ultimately no significant difference in diagnostic accuracy. However, when iodine quantification was used with a threshold of 2 mg/ml sensitivity was highest with still very good specificity resulting in overall the best diagnostic accuracy of 92.8 %. The finding that iodine quantification (mg/ml) is superior to iodine enhancement (HU) measurements for the correct depiction of lesion vascularity is supported and confirmed by Ascenti et al. [53] and Mileto et al. [54]. Accuracy could be increased up to 97 % in 52 patients with 72 lesions. Seven from 19 lesions that were deemed equivocal on classic HU-based criteria and were pathologically proven RCC could be reliable classified as such with the quantitative approach. In cysts with pseudo-enhancement, the phenomenon could be identified as such by quantitative iodine measurements. While the 2 mg/ml threshold was determined empirically in Kaza's study population, Ascenti's and Mileto's 0.5 mg/ml threshold was based on results of a prior phantom study. Differences in scanner technology, scan delay, and contrast protocol are potential confounding factors. However, when we look closer to the average iodine content of enhancing lesions, it was around 2.2 mg/ml in the DS DECT groups, which lays more in the proximity of Kaza's findings. Independent from the approach, iodine quantification seems to have the potential to actually boost diagnostic performance of renal CT. Just recently Mileto et al. published on the potential of virtual mono-chromatic images to overcome renal cyst pseudoenhancement [55]. This phenomenon did not occur when images were reconstructed with 80–90 keV, however they only looked into cysts >2 cm.

Urinary Tract

Unlike contrast-enhanced dual-energy applications in the abdomen, scans for urinary tract stone differentiation are carried out primarily un-enhanced. The material decomposition algorithms used take are based on urine/water, calcium (as most of the stones will show some sort of calcium component) and uric acid (being responsible for a substantial amount of stones) as the basic discriminators. Uric acid is somewhat ideal to be differentiated from other stone types as it contains no elements with high atomic number. And coincidentally, the metaphylaxis of uric acid stones is different to that of other stone types. However, in the acute setting when a patient presents with flank paint, colic, or hematuria straight forward treatment for symptom relief (i.e., pain relief with stone extraction and stent placement) will be sought depending on stone size and location irrespective of the stone composition. In patients with larger, immobile calculi in the renal pelvis or recurrent complaints different strategies apply and here is where stone differentiation is of added value for choosing the right treatment. Broad-based evidence is available that irrespective of the scanner technology reliable differentiation of uric acid and non-uric acid stones in patients is possible with almost 100 % accuracy [56–63]. Literature is not consistent in terms of further sub-classification of non-uric acid stones [56–63]. Limitations of the technique include high image noise e.g., in obese patients or small stones <3 mm that may be mapped falsely. Examination strategies include a low-dose single-energy screening scan followed by a short DE spiral or selecting primarily a low-dose DE protocol as suggested by Thomas et al. [61, 62] with equal accuracy. Jepperson et al. were able to show that DE-based stone evaluation is more accurate, faster to learn, and easier to interpret than HU-based evaluation across a cohort of 14 physicians of various experience levels [64••].

CT urography is a widely used test with high diagnostic power in patients with macro- or micro-hematuria. TUE images are important to detect stones and calcifications, blood, infection, or to help with renal lesion characterization. Attempts have been made with DECT to replace TUE with VUE images derived from excretory phase or mixed

nephrographic-excretory phase with split-bolus contrast injection. Although the application of low contrast volumes [65], urine dilution with furosemide [66] or a 100/140 Sn kV configuration [67] seem to increase stone detection rates and reduce incomplete iodine subtraction in the collection systems that may mask small concrements, the overall diagnostic accuracy for the reliable detection of small calculi is significantly inferior to TUE series [68, 69•, 70, 71]. Hence, the conclusion can be made, that VUE images in CT urography cannot replace a TUE series if robust and reliable diagnosis is to be established. Determinants of poor stone detection rate are stone size of 3 mm or less, low stone attenuation, high image noise, and high iodine density in the urinary tract.

Tumor Vitality and Response Assessment

One of the most exciting fields for DECT for sure is oncological imaging. Besides improving lesion detectability by utilizing low photon energies in contrast-enhanced scans as exemplarily shown above, this includes more sophisticated and advanced tools such as iodine quantification of a tumor volume for response assessment or early detection of local recurrence after thermo-ablation by selectively looking at iodine-related enhancement. Since iodine quantity can be seen as a surrogate parameter of blood supply and consequently of tumor perfusion, the ideal lesion for these types of applications enhances well [e.g., hepatocellular carcinoma (HCC), renal cell carcinoma (RCC), neuroendocrine tumors (NET), gastrointestinal stroma tumors (GIST)]. For reproducible and reliable results in the follow-up, a contrast-injection protocol tailored to patient-specific parameters—mostly this will be a weight-based protocol—and normalization of contrast to the input vessel (e.g., aorta) are mandatory.

One of the earliest experiences with iodine quantification was reported by Apfaltrer et al. in 24 patients with GIST under tyrosine kinase inhibitor treatment examined on a first-generation DS DECT [72]. They found excellent correlation of iodine-related attenuation values and Choi criteria. From the same group, Meyer et al. were the first to present survival data in 17 GIST patients under tyrosine kinase inhibitor therapy [73•]. Besides RECIST and Choi criteria, a newly developed DECT score taking iodine-related attenuation and size change into account were correlated to survival. DECT criteria classified response similar to RECIST, but was the only criterion at 6 month follow-up to predict overall survival. Dai et al. recently compared early response of HCC to sorafenib treatment in 15 patients according to AASLD and Choi criteria ,and correlated volumetric total tumor iodine uptake [74]. Iodine uptake was in line with AASLD criteria with no relevant shift of response group (tumor control vs. progression). The authors used a second-generation DS DECT scanner and a bodyweight-adapted contrast protocol. They concluded that volume iodine measurement may present the more reliable and easier to perform measure of tumor response in HCC. Uhrig et al. published a more technically orientated paper on combined semi-automated RECIST and volumetric iodine uptake measurement in nine patients with metastatic malignant melanoma and vemurafenib treatment [75]. They showed that volumetric iodine uptake decreased much more than RECIST in responders.

The studies listed here can be seen as first experience papers in the field. Given the tremendous socio-economic importance of cancer in general not only in the Western world, but also of HCC in particular in Asia the impact of these first findings will become clear when large-scale prospective therapy studies are launched, dedicatedly designed for DECT-based response parameters.

Patients after local thermo-ablation undergo regular restaging or post-interventional control scans to document complete or incomplete tumor ablation and to detect local recurrence early. The necrosis zone is a dynamic tissue showing typical changes of its appearance days, months, and years after ablation. And although one is familiar with these changes of shape, density, and contrast enhancement, the differentiation of reactive enhancement caused by granulation tissue and repair processes from early recurrence or incomplete tumor ablation may sometimes be challenging. Park et al. could not observe a benefit of iodine maps over standard linearly blended gray scale images for the detection of recurrent RCC after kidney radiofrequency ablation (RFA) with a second-generation DS DECT [76]. A major limitation is that only 4 of 47 patients had recurrence which per se limits the significance of the results. Lee et al. used a DS DECT scanner of the first generation to look at liver ablation areas (75 patients, mostly HCC) [77]. Seven VUE image series were rated unacceptable due to small FOV with incomplete coverage of the liver, misregistration artifacts, and lipiodol subtraction. Iodine maps and iodine-related density on the other side were seen as a helpful add-on since they revealed a more homogeneous appearance of the necrosis without influence by hemorrhage or detritus. Also in this cohort, only three patients developed recurrence giving the same limitation as mentioned above. Lee et al. dealt with the problem that HCC progression or recurrence after transarterial chemoembolization (TACE) may be difficult to diagnose due to remaining hyperdense lipiodol retentions [78]. They developed special window settings and thresholds for iodine density maps to be best viewed with to maximize the contrast for tumor-related iodine enhancement and to minimize the effects of iodinated oil, which typically appears very dense. With their approach, they were able to improve the confidence of diagnosis. The number of decisions for definitive viable HCC was significantly increased while the number of uncertain

diagnosis was significantly decreased compared to standard CT images with higher interobserver agreement. Their work was also conducted on a first-generation DS DECT.

Conclusion and Outlook

DECT has emerged to a modality that has established itself in abdominal imaging because of advanced image analysis and availability of information that reach beyond simple morphological imaging of pathologies. The possibility of improved tissue differentiation and characterization has not only been appealing for researchers but has found a way in clinical routine imaging worldwide for making the right diagnosis faster with higher confidence without increased radiation exposure. Kidney stone differentiation and iodine overlay techniques are already used to streamline workflow and patient management. Since low noise source data are essential to obtain accurate DE-based postprocessing, application of DECT should be restricted to patients not exceeding a BMI of 35 kg/m^2. Currently, literature suggests that VUE images are largely similar in terms of diagnostic quality, but they do look substantially different and HU measurements may not be as accurate as TUE. Hence, they may not yet be an acceptable substitute for TUE in every case. As technology will advance, the quality of virtual un-enhanced images can be expected to improve, tissue differentiation to be more accurate and patient exposure to be further lowered. For the authors, oncological applications for early detection and therapy monitoring present the most exciting field of DECT. The initial experiences of some working groups presented here are the first steps in a sector with growing socio-economic importance. Their true impact will have to be investigated in prospective multi-center studies.

Compliance with Ethics Guidelines

Conflict of Interest Dr. Ralf W. Bauer reports grants and personal fees from Siemens Healthcare and personal fees from GE Healthcare. Dr. Sebastian Fischer declares no potential conflicts of interest.

Human and Animal Rights and Informed Consent This article does not contain any studies with human or animal subjects performed by any of the authors.

References

Recently published papers of particular interest have been highlighted as:
- • Of importance
- •• Of major importance

1. • Johnson TR. Dual-energy CT: general principles. AJR Am J Roentgenol 2012;199:S3–8. *This paper gives a state-of-the-art insight into physics and technical aspects of Dual-Energy CT of all available systems.*
2. Johnson TR, Krauss B, Sedlmair M, et al. Material differentiation by dual energy CT: initial experience. Eur Radiol. 2007;17:1510–7.
3. Guimaraes LS, Fletcher JG, Harmsen WS, et al. Appropriate patient selection at abdominal dual-energy CT using 80 kV: relationship between patient size, image noise, and image quality. Radiology. 2010;257:732–42.
4. Primak AN, Giraldo JC, Eusemann CD, et al. Dual-source dual-energy CT with additional tin filtration: dose and image quality evaluation in phantoms and in vivo. AJR Am J Roentgenol. 2010;195:1164–74.
5. Im AL, Lee YH, Bang DH, Yoon KH, Park SH. Dual energy CT in patients with acute abdomen; is it possible for virtual non-enhanced images to replace true non-enhanced images? Emerg Radiol. 2013;20:475–83.
6. •• Grant KL, Flohr TG, Krauss B, Sedlmair M, Thomas C, Schmidt B. Assessment of an advanced image-based technique to calculate virtual monoenergetic computed tomographic images from a dual-energy examination to improve contrast-to-noise ratio in examinations using iodinated contrast media. Invest Radiol 2013;49:586–92. *The prinicples behind pseudo-mono-energetic image generation are explained in detail and illustrated with graphics and examples.*
7. Yu L, Leng S, McCollough CH. Dual-energy CT-based monochromatic imaging. AJR Am J Roentgenol. 2012;199:S9–15.
8. De Cecco CN, Darnell A, Macias N, et al. Second-generation dual-energy computed tomography of the abdomen: radiation dose comparison with 64- and 128-row single-energy acquisition. J Comput Assist Tomogr. 2013;37:543–6.
9. Purysko AS, Primak AN, Baker ME, et al. Comparison of radiation dose and image quality from single-energy and dual-energy CT examinations in the same patients screened for hepatocellular carcinoma. Clin Radiol. 2014. doi:10.1016/j.crad.2014.08.021.
10. Zhang LJ, Peng J, Wu SY, et al. Liver virtual non-enhanced CT with dual-source, dual-energy CT: a preliminary study. Eur Radiol. 2010;20:2257–64.
11. De Cecco CN, Buffa V, Fedeli S, et al. Dual energy CT (DECT) of the liver: conventional versus virtual unenhanced images. Eur Radiol. 2010;20:2870–5.
12. De Cecco CN, Darnell A, Macias N, et al. Virtual unenhanced images of the abdomen with second-generation dual-source dual-energy computed tomography: image quality and liver lesion detection. Invest Radiol. 2013;48:1–9.
13. •• Sahni VA, Shinagare AB, Silverman SG. Virtual unenhanced CT images acquired from dual-energy CT urography: accuracy of attenuation values and variation with contrast material phase. Clin Radiol 2013;68:264–71. *This paper very nicely shows the strenghts and weaknesses of virtual un-enhanced images/iodine subtraction techniques with respect to HU accuracy, image artifacts and kidney stone detection.*
14. Barrett T, Bowden DJ, Shaida N, et al. Virtual unenhanced second generation dual-source CT of the liver: is it time to discard the conventional unenhanced phase? Eur J Radiol. 2012;81:1438–45.
15. Toepker M, Moritz T, Krauss B, et al. Virtual non-contrast in second-generation, dual-energy computed tomography: reliability of attenuation values. Eur J Radiol. 2012;81:e398–405.
16. Kaufmann S, Sauter A, Spira D, et al. Tin-filter enhanced dual-energy-CT: image quality and accuracy of CT numbers in virtual noncontrast imaging. Acad Radiol. 2013;20:596–603.
17. Miller CM, Gupta RT, Paulson EK, et al. Effect of organ enhancement and habitus on estimation of unenhanced attenuation at contrast-enhanced dual-energy MDCT: concepts for individualized and organ-specific spectral iodine subtraction strategies. AJR Am J Roentgenol. 2011;196:W558–64.

18. Gao SY, Zhang XP, Cui Y, et al. Fused monochromatic imaging acquired by single source dual energy CT in hepatocellular carcinoma during arterial phase: an initial experience. Chin J Cancer Res. 2014;26:437–43.
19. • Lv P, Lin XZ, Chen K, Gao J. Spectral CT in patients with small HCC: investigation of image quality and diagnostic accuracy. Eur Radiol 2012;22:2117–24. *The authors show how diagnostic accuracy for small hyperenhancing liver lesions can be improved by virtual mono-energetic images at low keV.*
20. Shuman WP, Green DE, Busey JM, et al. Dual-energy liver CT: effect of monochromatic imaging on lesion detection, conspicuity, and contrast-to-noise ratio of hypervascular lesions on late arterial phase. AJR Am J Roentgenol. 2014;203:601–6.
21. Yamada Y, Jinzaki M, Tanami Y, Abe T, Kuribayashi S. Virtual monochromatic spectral imaging for the evaluation of hypovascular hepatic metastases: the optimal monochromatic level with fast kilovoltage switching dual-energy computed tomography. Invest Radiol. 2012;47:292–8.
22. Kim KS, Lee JM, Kim SH, et al. Image fusion in dual energy computed tomography for detection of hypervascular liver hepatocellular carcinoma: phantom and preliminary studies. Invest Radiol. 2010;45:149–57.
23. Li S, Wang C, Jiang X, Xu G. Effects of dual-energy CT with non-linear blending on abdominal CT angiography. Korean J Radiol. 2014;15:430–8.
24. Lv P, Liu J, Wu R, Hou P, Hu L, Gao J. Use of non-linear image blending with dual-energy CT improves vascular visualization in abdominal angiography. Clin Radiol. 2014;69:e93–9.
25. Schabel C, Bongers M, Sedlmair M, et al. Assessment of the hepatic veins in poor contrast conditions using dual energy CT: evaluation of a novel monoenergetic extrapolation software algorithm. RoFo. 2014;186:591–7.
26. Wang Q, Shi G, Liu X, Wu R, Wang S. Optimal contrast of computed tomography portal venography using dual-energy computed tomography. J Comput Assist Tomogr. 2013;37:142–8.
27. Zhao LQ, He W, Li JY, Chen JH, Wang KY, Tan L. Improving image quality in portal venography with spectral CT imaging. Eur J Radiol. 2012;81:1677–81.
28. Clark ZE, Bolus DN, Little MD, Morgan DE. Abdominal rapid-kVp-switching dual-energy MDCT with reduced IV contrast compared to conventional MDCT with standard weight-based IV contrast: an intra-patient comparison. Abdom Imaging. 2014. doi:10.1007/s00261-014-0253-3.
29. •• Mileto A, Ramirez-Giraldo JC, Marin D, et al. Nonlinear image blending for dual-energy MDCT of the abdomen: can image quality be preserved if the contrast medium dose is reduced? AJR Am J Roentgenol 2014;203:838–45. *The authors were able to show that adequate selection of non-linear blending settings holds the potential for reducing the total required contrast material dose without loss of image quality for portal venous phase CT.*
30. Patel BN, Kumbla RA, Berland LL, Fineberg NS, Morgan DE. Material density hepatic steatosis quantification on intravenous contrast-enhanced rapid kilovolt (peak)-switching single-source dual-energy computed tomography. J Comput Assist Tomogr. 2013;37:904–10.
31. Zheng X, Ren Y, Phillips WT, et al. Assessment of hepatic fatty infiltration using spectral computed tomography imaging: a pilot study. J Comput Assist Tomogr. 2013;37:134–41.
32. Joe E, Kim SH, Lee KB, et al. Feasibility and accuracy of dual-source dual-energy CT for noninvasive determination of hepatic iron accumulation. Radiology. 2011;262:126–35.
33. Bauer RW, Schulz JR, Zedler B, Graf TG, Vogl TJ. Compound analysis of gallstones using dual energy computed tomography—results in a phantom model. Eur J Radiol. 2010;75:e74–80.
34. Voit H, Krauss B, Heinrich MC, et al. Dual-source CT: in vitro characterization of gallstones using dual energy analysis. RoFo. 2009;181:367–73.
35. Sommer CM, Schwarzwaelder CB, Stiller W, et al. Dual-energy computed-tomography cholangiography in potential donors for living-related liver transplantation: initial experience. Invest Radiol. 2010;45:406–12.
36. Stiller W, Schwarzwaelder CB, Sommer CM, Veloza S, Radeleff BA, Kauczor HU. Dual-energy, standard and low-kVp contrast-enhanced CT-cholangiography: a comparative analysis of image quality and radiation exposure. Eur J Radiol. 2012;81:1405–12.
37. Mileto A, Mazziotti S, Gaeta M, et al. Pancreatic dual-source dual-energy CT: is it time to discard unenhanced imaging? Clin Radiol. 2012;67:334–9.
38. Patel BN, Thomas JV, Lockhart ME, Berland LL, Morgan DE. Single-source dual-energy spectral multidetector CT of pancreatic adenocarcinoma: optimization of energy level viewing significantly increases lesion contrast. Clin Radiol. 2013;68:148–54.
39. • Lin XZ, Wu ZY, Tao R, et al. Dual energy spectral CT imaging of insulinoma-value in preoperative diagnosis compared with conventional multi-detector CT. Eur J Radiol 2012;81:2487–94. *The combination of virtual mono-chromatic images at low keV and iodine maps can substantially increase the detection rate of small pancreatic insulinoma over standard MDCT.*
40. Gnannt R, Fischer M, Goetti R, Karlo C, Leschka S, Alkadhi H. Dual-energy CT for characterization of the incidental adrenal mass: preliminary observations. AJR Am J Roentgenol. 2012;198:138–44.
41. Ho LM, Marin D, Neville AM, et al. Characterization of adrenal nodules with dual-energy CT: can virtual unenhanced attenuation values replace true unenhanced attenuation values? AJR Am J Roentgenol. 2011;198:840–5.
42. Kim YK, Park BK, Kim CK, Park SY. Adenoma characterization: adrenal protocol with dual-energy CT. Radiology. 2013;267:155–63.
43. Gupta RT, Ho LM, Marin D, Boll DT, Barnhart HX, Nelson RC. Dual-energy CT for characterization of adrenal nodules: initial experience. AJR Am J Roentgenol. 2010;194:1479–83.
44. • Shi JW, Dai HZ, Shen L, Xu DF. Dual-energy CT: clinical application in differentiating an adrenal adenoma from a metastasis. Acta Radiol 2014;55:505–12. *A well powered study on how DECT can help with the differentiation of adrenal adenoma from metastases. Adenomas show attenuation characteristics at high and low photon energies that are substantially different from metastases.*
45. Morgan DE, Weber AC, Lockhart ME, Weber TM, Fineberg NS, Berland LL. Differentiation of high lipid content from low lipid content adrenal lesions using single-source rapid kilovolt (peak)-switching dual-energy multidetector CT. J Comput Assist Tomogr. 2013;37:937–43.
46. Mileto A, Nelson RC, Marin D, Choudhury KR, Ho LM. Dual-energy multidetector CT for the characterization of incidental adrenal nodules: diagnostic performance of contrast-enhanced material density analysis. Radiology. 2014. doi:10.1148/radiol.14140876:140876.
47. Graser A, Johnson TR, Hecht EM, et al. Dual-energy CT in patients suspected of having renal masses: can virtual nonenhanced images replace true nonenhanced images? Radiology. 2009;252:433–40.
48. Neville AM, Gupta RT, Miller CM, Merkle EM, Paulson EK, Boll DT. Detection of renal lesion enhancement with dual-energy multidetector CT. Radiology. 2011;259:173–83.
49. •• Graser A, Becker CR, Staehler M, et al. Single-phase dual-energy CT allows for characterization of renal masses as benign or malignant. Invest Radiol 2010;45:399–405. *The authors were able to demonstrate in a large patient cohort that with the help of DE-specific postprocessing with VUE and iodine maps an*

accurate diagnosis of renal lesions can be made faster with less radiation exposure.

50. Song KD, Kim CK, Park BK, Kim B. Utility of iodine overlay technique and virtual unenhanced images for the characterization of renal masses by dual-energy CT. AJR Am J Roentgenol. 2011;197:W1076–82.
51. Ascenti G, Mazziotti S, Mileto A, et al. Dual-source dual-energy CT evaluation of complex cystic renal masses. AJR Am J Roentgenol. 2012;199:1026–34.
52. • Kaza RK, Caoili EM, Cohan RH, Platt JF. Distinguishing enhancing from nonenhancing renal lesions with fast kilovoltage-switching dual-energy CT. AJR Am J Roentgenol 2011;197: 1375–1381. *A quantitative approach to determine the iodine-related enhancement of a renal lesion. A threshold of 2 mg/ml was ideal to discriminate enhancement from no enhancement.*
53. Ascenti G, Mileto A, Krauss B, et al. Distinguishing enhancing from nonenhancing renal masses with dual-source dual-energy CT: iodine quantification versus standard enhancement measurements. Eur Radiol. 2013;23:2288–95.
54. Mileto A, Marin D, Ramirez-Giraldo JC, et al. Accuracy of contrast-enhanced dual-energy MDCT for the assessment of iodine uptake in renal lesions. AJR Am J Roentgenol. 2014;202: W466–74.
55. Mileto A, Nelson RC, Samei E, et al. Impact of dual-energy multi-detector row CT with virtual monochromatic imaging on renal cyst pseudoenhancement: in vitro and in vivo study. Radiology. 2014;272:767–76.
56. Graser A, Johnson TR, Bader M, et al. Dual energy CT characterization of urinary calculi: initial in vitro and clinical experience. Invest Radiol. 2008;43:112–9.
57. Hidas G, Eliahou R, Duvdevani M, et al. Determination of renal stone composition with dual-energy CT: in vivo analysis and comparison with X-ray diffraction. Radiology. 2010;257:394–401.
58. Kulkarni NM, Eisner BH, Pinho DF, Joshi MC, Kambadakone AR, Sahani DV. Determination of renal stone composition in phantom and patients using single-source dual-energy computed tomography. J Comput Assist Tomogr. 2013;37:37–45.
59. Manglaviti G, Tresoldi S, Guerrer CS, et al. In vivo evaluation of the chemical composition of urinary stones using dual-energy CT. AJR Am J Roentgenol. 2011;197:W76–83.
60. Stolzmann P, Kozomara M, Chuck N, et al. In vivo identification of uric acid stones with dual-energy CT: diagnostic performance evaluation in patients. Abdom Imaging. 2009;35:629–35.
61. Thomas C, Heuschmid M, Schilling D, et al. Urinary calculi composed of uric acid, cystine, and mineral salts: differentiation with dual-energy CT at a radiation dose comparable to that of intravenous pyelography. Radiology. 2010;257:402–9.
62. Thomas C, Patschan O, Ketelsen D, et al. Dual-energy CT for the characterization of urinary calculi: in vitro and in vivo evaluation of a low-dose scanning protocol. Eur Radiol. 2009;19:1553–9.
63. Zilberman DE, Ferrandino MN, Preminger GM, Paulson EK, Lipkin ME, Boll DT. In vivo determination of urinary stone composition using dual energy computerized tomography with advanced post-acquisition processing. J Urol. 2010;184:2354–9.
64. •• Jepperson MA, Ibrahim el SH, Taylor A, Cernigliaro JG, Haley WE, Thiel DD. Accuracy and efficiency of determining urinary calculi composition using dual-energy computed tomography compared with Hounsfield unit measurements for practicing physicians. Urology 2014;84:561–64. *A highly interesting study that focuses on the ease of use, learing curve, reproduceability and reliability of DE-based kidney stone characterization among non-radiologists.*
65. Toepker M, Kuehas F, Kienzl D, et al. Dual energy computerized tomography with a split bolus—a 1-stop shop for patients with suspected urinary stones? J Urol. 2013;191:792–7.
66. Botsikas D, Hansen C, Stefanelli S, Becker CD, Montet X. Urinary stone detection and characterisation with dual-energy CT urography after furosemide intravenous injection: preliminary results. Eur Radiol. 2014;24:709–14.
67. Karlo CA, Gnannt R, Winklehner A, et al. Split-bolus dual-energy CT urography: protocol optimization and diagnostic performance for the detection of urinary stones. Abdom Imaging. 2013;38:1136–43.
68. Lv P, Zhang Y, Liu J, Ji L, Chen Y, Gao J. Material decomposition images generated from spectral CT: detectability of urinary calculi and influencing factors. Acad Radiol. 2014;21:79–85.
69. • Mangold S, Thomas C, Fenchel M, et al. Virtual nonenhanced dual-energy CT urography with tin-filter technology: determinants of detection of urinary calculi in the renal collecting system. Radiology 2012;264:119–25. *A thoroughly conducted methodic study to analyise influencing factors for urinary tract calculi detection rate on VUE images derived from DECT urography.*
70. Moon JW, Park BK, Kim CK, Park SY. Evaluation of virtual unenhanced CT obtained from dual-energy CT urography for detecting urinary stones. Br J Radiol. 2012;85:e176–81.
71. Takahashi N, Vrtiska TJ, Kawashima A, et al. Detectability of urinary stones on virtual nonenhanced images generated at pyelographic-phase dual-energy CT. Radiology. 2010;256:184–90.
72. Apfaltrer P, Meyer M, Meier C, et al. Contrast-enhanced dual-energy CT of gastrointestinal stromal tumors: is iodine-related attenuation a potential indicator of tumor response? Invest Radiol. 2012;47:65–70.
73. • Meyer M, Hohenberger P, Apfaltrer P, et al. CT-based response assessment of advanced gastrointestinal stromal tumor: dual energy CT provides a more predictive imaging biomarker of clinical benefit than RECIST or Choi criteria. Eur J Radiol 2013;82:923–28. *Outcome study on GIST under therapy followed-up with DECT. This is the first article to show that only DE-specific information can be reliable predictors for surivial.*
74. Dai X, Schlemmer HP, Schmidt B, et al. Quantitative therapy response assessment by volumetric iodine-uptake measurement: initial experience in patients with advanced hepatocellular carcinoma treated with sorafenib. Eur J Radiol. 2013;82:327–34.
75. Uhrig M, Sedlmair M, Schlemmer HP, Hassel JC, Ganten M. Monitoring targeted therapy using dual-energy CT: semi-automatic RECIST plus supplementary functional information by quantifying iodine uptake of melanoma metastases. Cancer Imaging. 2013;13:306–13.
76. Park SY, Kim CK, Park BK. Dual-energy CT in assessing therapeutic response to radiofrequency ablation of renal cell carcinomas. Eur J Radiol. 2014;83:e73–9.
77. Lee SH, Lee JM, Kim KW, et al. Dual-energy computed tomography to assess tumor response to hepatic radiofrequency ablation: potential diagnostic value of virtual noncontrast images and iodine maps. Invest Radiol. 2011;46:77–84.
78. Lee JA, Jeong WK, Kim Y, et al. Dual-energy CT to detect recurrent HCC after TACE: initial experience of color-coded iodine CT imaging. Eur J Radiol. 2013;82:569–76.